

THE EXPERIMENTAL STUDIES OF HEAT TRANSFER AND FRICTION

FACTOR IN A ROUGHENED SOLAR AIR HEATER

USING ARC RIB GEOMETRIES

SANJEEV KUMAR YADAV¹ & ATUL LANJEWAR²

¹Research Scholar, Department of Mechanical Engineering,

Maulana Azad National Institute of Technology, Bhopal, Madhya Pradesh, India

²Associate Professor, Department of Mechanical Engineering,

Maulana Azad National Institute of Technology, Bhopal, Madhya Pradesh, India

ABSTRACT

Solar air heater utilizes rib roughness to enhance heat transfer. Experimental investigation has been conducted to study heat transfer and efficiency improvement in solar air heater using the arc rib roughness. Rib roughness has relative roughness pitch of 10, rib height is 2 mm and mass flow rate varies from 4000-14000. Heat transfer and efficiency improvement have been compared with smooth plate operating under similar flow conditions. Maximum enhancement in Nusselt number is 2.06, 2.25, 2.40 and 2.57 over a smooth plate for continuous arc, gap in a continuous arc, staggered element in broken arc rib and for proposed new arc rib geometry namely multi staggered element in broken arc respectively. Maximum thermo-hydraulic parameter amongst all arc rib geometries studied is reported as 1.70 for proposed new arc rib geometry.

KEYWORDS: Solar Air Heater, Heat Transfer, Arc Rib Roughness, Efficiency & New Arc Rib Geometry

Received: Dec 15, 2018; **Accepted:** Jan 15, 2019; **Published:** Feb 06, 2019; **Paper Id.:** IJMPERDAPR20199

1. INTRODUCTION

Solar air heater due to its simple design and low operation and maintenance cost is widely used as a solar collector. The thermal performance of solar air heater is low due to its poor heat transfer capacity between absorber plate and the working fluid i.e. air. The use of artificial roughness on absorber surface is an effective method of heat transfer augmentation between absorber plate and working fluid. The roughness element breaks the thermal boundary layer causing heat transfer augmentation. However this also increases friction loss leading to the rise in pumping power requirement from blower or fan. To minimize the friction loss and pumping power the turbulence should be created at the vicinity of absorber surface so that laminar sub-layer is broken.

The earliest investigations to determine the effect of roughness on the flow was done by Nikuradse [1]. Several investigators [2-5] developed the laws related to friction and heat transfer in rough pipes. Han [6] performed an experimental evaluation of fully developed air flow in a square duct roughened with two opposite walls. Prasad and Mullick [7] used small diameter wire as artificial roughness in solar air heater absorber plate. Prasad and Saini [8] determined effect of relative roughness height (e/D_h) and relative roughness pitch (p/e) on heat transfer and friction factor using circular cross section wire as artificial roughness. They reported an increase in friction by 6.3% and decrease in heat transfer by 10.7% with increase in relative roughness height. Some of the

notable researchers are Saini and Saini [9], Gupta et al. [10], Varshney and Saini [11], Karwa et al. [12, 13], Bhagoria et al. [14], Momin et al. [15], Sahu and Bhagoria [16], Karwa [17], Jaurkar et al. [18], Aharwal et al. [19] and Varun et al. [20]. They used different roughness geometries for the heat transfer enhancement.

Saini and Saini [21] used continuous arc rib roughness to evaluate heat transfer and friction factor performance of solar air heater. They reported maximum enhancement in Nusselt number by 3.8 times that of the smooth duct for arc angle ($\alpha/90$) as 0.3333, relative roughness height (e/D_h) 0.0422, however the friction factor increased by 1.75 corresponding to the same parameters. They also developed correlations for Nusselt number and friction factor. Hans et al. [22] investigated artificial roughness by providing gap in continuous arc roughness. The parameters encompassed relative roughness pitch (p/e) 4-12, relative roughness height (e/D_h) 0.022-0.043, arc angle (α) 15-75°, relative gap width (g/e) 0.5-2.5, relative gap position (d/W) 0.2-0.8 and Reynolds number (Re) 2000-16000. The authors reported maximum enhancement in Nusselt number and friction factor as 2.63 and 2.44 times, respectively that of a smooth absorber plate and 1.19 and 1.14 times compared with full arc rib roughness for relative roughness pitch (p/e) 10, relative gap width (g/e) 1, relative gap position (d/W) 0.65, arc angle (α) 30° and relative roughness height 0.043. They also developed correlations for Nusselt number and friction factor. Gill et al. [23] used staggered element in broken arc rib roughness absorber plate of solar air heater. The parameter investigated were relative staggered rib size (r/e) as 1-6 for Reynolds number range (Re) 2000-16000. Other roughness parameters such as relative roughness pitch (p/e), arc, angle ($\alpha/90$), relative gap position (d/W), relative gap width (g/e) and relative roughness height (e/D_h) were kept constant. They reported enhancement in Nusselt number and friction factor by 3.6 and 2.5 times, respectively as compared to smooth duct and 2.6 and 2.27 times that of the broken arc without staggered element for relative staggered rib size (r/e) as 4. The present investigation is taken up to see the effect on heat transfer enhancement for a reduced aspect ratio of the duct. Aspect ratio in all previous studies is 12 and in present investigation aspect ratio is kept as 8. Also new arc rib geometry is proposed as an improvement over previous arc rib geometries and its performance is compared with previous arc rib geometries under similar flow and geometrical conditions. Roughness parameters for previous arc rib geometries are kept based on their optimum values reported in literature.

2. ROUGHNESS GEOMETRY AND RANGE OF PARAMETERS

To investigate the performance of various arc rib geometries an open loop indoor test setup is designed and fabricated as per ASHRAE [24]. In the present experimental investigation of artificially roughened solar air heater heat transfer analysis for various arc rib geometries is considered for investigation. Plate photograph of different arc rib roughness geometry is shown in Figure 1. The roughness parameter for investigation of new arc rib geometry namely the multi staggered element in broken arc rib is shown in Table 1. Insulated copper wires of circular cross section have been used to create rib roughness. In the present investigation four arc shaped roughness geometries have been evaluated i.e. Continuous arc [21], gap in a continuous arc [22], staggered element in broken arc rib [23] and new arc rib geometry namely multi staggered element in broken arc rib. These geometries are shown in Figure 1 as A, B, C and D respectively.

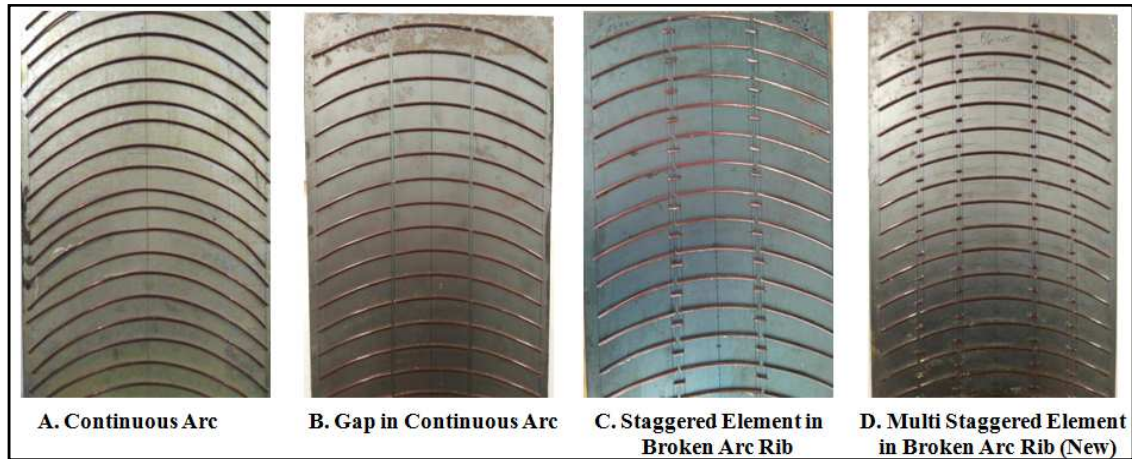


Figure 1: Photograph of Various Arc Rib Roughness Geometries

Table 1: Range of Parameters for New Arc Roughness Geometry

S. No.	Name of Parameter	Value
1	Diameter of wire (e)	2mm
2	Relative roughness pitch (p/e)	10
3	Relative roughness height (e/D _h)	0.045
4	Range of Reynolds number (Re)	3000-15000
5	Angle of attack of arc (α)	30°
6	Number of gaps on each side of arc	2
7	Relative gap width (g/e)	1
8	Relative staggered rib size (r/e)	4.5
9	Relative staggered rib pitch (p'/p)	0.4
10	Duct aspect ratio	8

3. EXPERIMENTAL SETUP

The experimental setup is shown in Figure 2. It consists of a rectangular test section, converging section, circular pipe having an orifice plate to measure flow rate, blower and electric motor. A variac is used to control voltage and current to supply heat flux to the absorber plate. Ammeter and voltmeter are used to measure current and voltage respectively supplied to heater. Thermocouple wires are fitted at inlet, outlet and over the plate to measure inlet, outlet and plate temperature. An electronic data logging device is used to determine the temperature at real time. A U-tube manometer is used to measure pressure drop across the orifice plate. Pressure drop along the plate is measured with an electronic pressure metre.

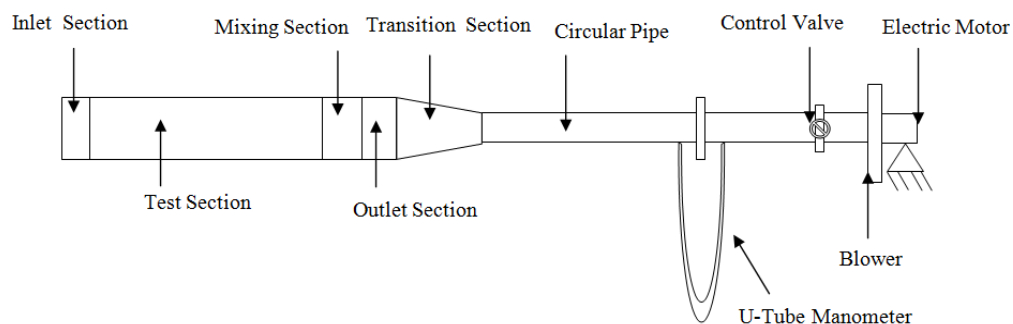


Figure 2: Schematic of Experimental Set-up

4. DATA REDUCTION

The values of air and plate temperature were measured for a constant heat flux and mass flow rate in a steady state. Heat transfer, friction factor and Nusselt number have been calculated from data obtained. This helps find the effect of various parameters on Nusselt number and friction factor using following formulae.

$$Q = m \times C_p \times (T_o - T_i) \quad (1)$$

$$h = Q / [A_p \times (T_p - T_f)] \quad (2)$$

$$Nu_r = (h \times D_h) / k \quad (3)$$

$$f_r = D_h \times \Delta P / (2 \times L \times V^2 \times \rho) \quad (4)$$

$$\eta = Q / (I \times A_p) \quad (5)$$

5. RESULTS

5.1. Validity Test

Nusselt number and friction factor determined from the experiment performed on a smooth duct were compared with those obtained from the modified Dittus Boelter equation for Nusselt number and modified Blasius equation for friction factor. These theoretical equations are given as

Modified Blasius equation

$$f_s = 0.085 Re^{-0.25} \quad (6)$$

Modified Dittus Boelter equation

$$Nu_s = 0.023 Re^{0.8} Pr^{0.4} \quad (7)$$

where f_s is friction factor for smooth duct, Re is Reynolds number, Nu_s is Nusselt number for smooth duct. Comparison of experimental and predicted values of Nusselt number and friction factor for smooth plate is shown in Figure 3 and Figure 4 respectively. It is observed that the values of friction factor and Nusselt number for smooth plate obtained by experiments agree reasonably good with the values predicted by eqn. (6) and eqn. (7) respectively. As experimental values of Nusselt number and friction factor are in reasonably close agreement to predicted values, the validity of experiment is ensured.

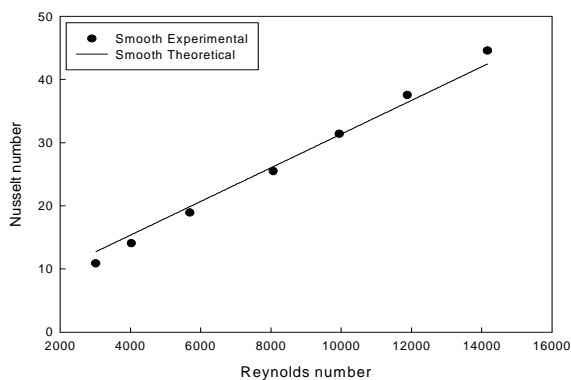


Figure 3: Comparison of Experimental and Theoretical Values of Nusselt Number for Smooth Plate

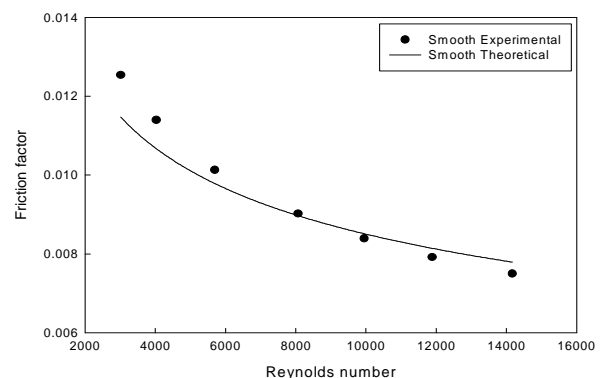


Figure 4: Comparison of Experimental and Theoretical Values of Friction Factor for Smooth Plate

5.2. Effect of Reynolds Number

Figure 5 shows the effect of Reynolds number on Nusselt number and Figure 6 shows the effect of Reynolds number on the friction factor for various arc rib geometries and for smooth plate. Nusselt number increases with Reynolds number and friction factor decreases with increase in Reynolds number. There is a large gap between smooth and arc roughened plate experimental data due to turbulence caused by rib roughness. The rib roughness brakes the laminar sub layer causing turbulence that promotes heat transfer. At lower Reynolds number the gap between the smooth and rough plate is less, but it is very significant for higher values of the Reynolds number.

Continuous arc roughness geometry of Saini and Saini [21] has a lowest Nusselt number over all arc rib geometries. Gap in continuous arc geometry of Hans et al. [22] has better heat transfer values as compared to continuous arc. This is due to flow acceleration through gap. Staggered element in broken arc rib geometry of Gill et al. [23] has better performance than rib geometry of Saini and Saini [21] and Hans et al. [22]. This is due to the combined effect of flow acceleration through the gap and flow scattering due to staggered rib. New arc roughness geometry namely the multi staggered element in broken arc rib has best performance as compared to all previous arc rib geometries studied till date. This is due to flow acceleration in gap and increase in scattered area flow due to providing multi staggered elements. Maximum enhancement in Nusselt number is 2.57 for new geometry whereas it is 2.40, 2.25 and 2.06 for staggered element in broken arc rib [23], gap in a continuous arc [22] and continuous arc roughness [21].

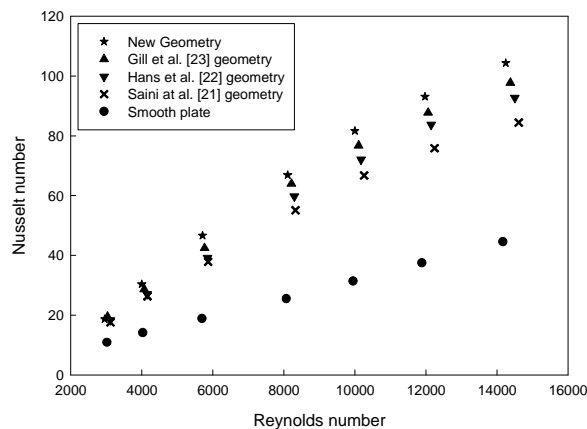


Figure 5: Variation of Nusselt Number with Reynolds Number for Various Arc Rib Geometries

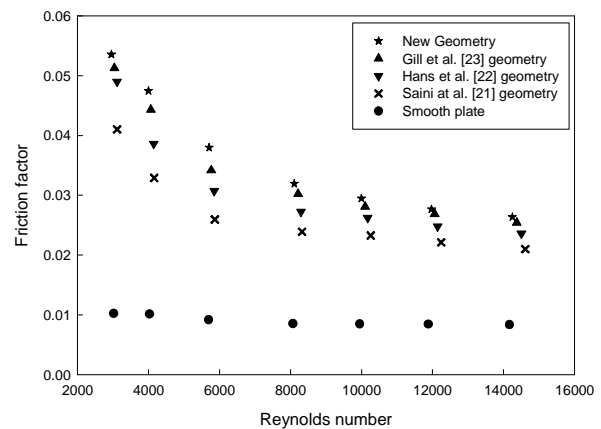


Figure 6: Variation of Friction Factor with Reynolds Number for Various Arc Rib Geometries

The variation of friction factor is along expected lines. Friction factor is lowest for continuous arc rib geometry of Saini and Saini [21]. Gap in continuous arc geometry of Hans et al. [22] has higher friction factor due to flow acceleration. Staggered element in broken arc rib of Gill et al. [23] has still a higher friction factor due to flow acceleration and scattering whereas new geometry namely multi staggered element in broken arc rib has highest friction factor due to greater scattering of flow and flow acceleration. The maximum increase in friction factor as compared to smooth plate is 4.64, 4.47, 4.31 and 3.61 respectively, for new geometry namely multi staggered element in broken arc rib, staggered element in broken arc rib, gap in continuous arc and continuous arc rib geometry respectively.

Figure 7 shows the variation of efficiency against Reynolds number of different arc rib geometries investigated. New geometry namely the multi staggered element in broken arc rib has the highest efficiency over all rib geometries considered.

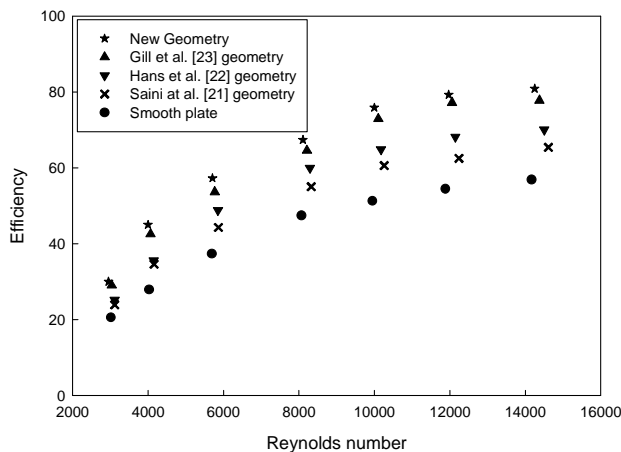


Figure 7: Variation of Thermal Efficiency with Reynolds Number for Various Arc Rib Geometries

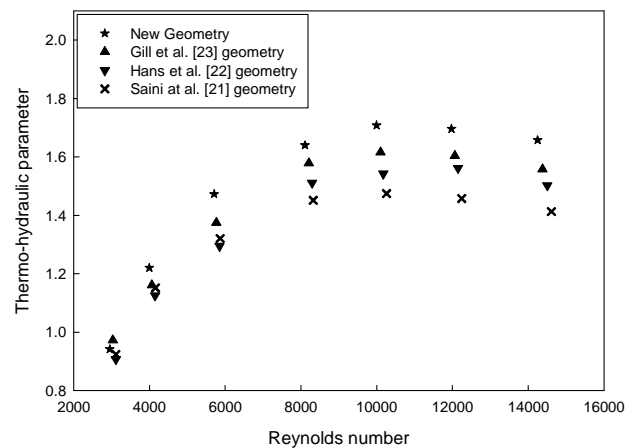


Figure 8: Variation of Thermo-Hydraulic Parameter with Reynolds Number for Various Arc Rib Geometries

5.3. Thermohydraulic Performance

The artificial roughness affects both Nusselt number and friction factor. The parameter that includes both Nusselt number and friction factor into consideration is Thermohydraulic performance (THP). It is given as below [3].

$$THP = (Nu_r/Nu_s)/(f_r/f_s)^{1/3} \quad (8)$$

Figure 8 shows effect of Reynolds number on Thermo-hydraulic performance parameter of roughness geometries investigated. New geometry namely multi staggered element in broken arc rib has highest THP value of 1.70 whereas it is 1.62, 1.56 and 1.47 for staggered element in broken arc, gap in continuous arc and continuous arc rib geometry respectively.

6. CONCLUSIONS

- The Nusselt number shows increasing trends with increasing Reynolds number. New geometry namely the multi staggered element in broken arc rib shows a maximum enhancement in Nusselt number as 2.57 times as compared to smooth plate.
- For a new geometry maximum increase in friction factor is 4.64 in comparison to smooth plate.
- Amongst all geometries studied new geometry has highest Thermo-hydraulic performance parameter. Maximum value for new geometry is 1.70 whereas it is 1.62, 1.56 and 1.47 for staggered element in broken arc, gap in continuous arc and continuous arc rib geometry respectively.
- Thermal efficiency also shows an increasing trend with an increase in Reynolds number
- Thermal efficiency is maximum for new geometry in comparison to other rib geometries studied till date.

NOMENCLATURE

A_p	Absorber plate surface area (m ²)	Q	Useful heat gain (W)
C_p	Specific heat of air (kJ/kgK)	r	Staggered rib length (m)
D_h	Hydraulic diameter (m)	r/e	Relative staggered rib length
d/W	Relative gap position	Re	Reynolds number
e	Rib height (m)	THP	Thermohydraulic parameter
e/D_h	Relative roughness height	T_f	Mean air flow temperature (°C)
f_r	Friction factor of rough plate	T_i	Inlet air temperature (°C)
f_s	Friction factor of smooth plate	T_o	Outlet air temperature (°C)
g	Gap width (m)	T_p	Plate temperature (°C)
g/e	Relative gap width	V	Velocity of air (m/s)
h	Convective heat transfer coefficient (W/m ² K)		
I	Heat flux (W/m ²)		
k	Thermal conductivity of air (W/mK)		
L	Plate length (m)		
m	Mass flow rate of air (kg/s)		
Nu_r	Nusselt number of rough plate		
Nu_s	Nusselt number of smooth plate		
p	Pitch (m)		
p'	Staggered rib pitch		
p/e	Relative roughness pitch		
p'/p	Relative staggered rib pitch		
Pr	Prandtl number		
ΔP	Pressure drop in duct (N/m ²)		

Greek Symbols

ρ	Density of air (kg/m ³)
α	Arc angle of attack (°)
η	Thermal efficiency

Subscripts

f	Flow
i	Inlet
o	Outlet
p	Plate
r	Rough
s	Smooth

REFERENCES

1. Nikuradse, J., (1950). *Laws of flow in rough pipes*, NACA Technical Memorandum, 1292.
2. Dipprey, D.F., &Sobersky, R.H.(1963). *Heat and momentum in smooth and rough tubes at various Prandtl numbers*. *Int. J. Heat Mass Transfer*, 60, 329-333.
3. Webb, R.L., Eckert, E.R.G., &Goldstein, R.J. (1971). *Heat transfer and friction in tubes with repeated rib roughness*. *Int. J. Heat Mass Transfer*, 14, 601-617
4. Bergles, A.E. (1988). *Some perspectives on enhanced heat transfer second generation heat transfer technology*. *J. Heat Transfer*, 110, 1082-1096.
5. Ravigururajan, T.S., &Bergles, A.E. (1994). *Visualization of flow phenomena near enhanced surfaces*. *J. Heat Transfer*, 116 (1), 54-57.
6. Han, J.C. (1984). *Heat transfer and friction in a channel with two opposite rib roughened walls*. *Trans. J. Heat Transfer*, 106, 774-781.
7. Prasad, B.N., &Mullick, S.C. (1983). *Heat transfer characteristics of solar air heater used for drying purposes*. *Applied Energy*, 13, 83-98.
8. Prasad, B.N., & Saini, J.S. (1988). *Effect of artificial roughness on heat transfer and friction factor in solar air heater*. *Solar Energy*, 41, 555-560.
9. Saini, R.P., & Saini, J.S. (1997). *Heat transfer and friction factor correlation for artificially roughened ducts with expanded metal mesh*. *Int. J. Heat Mass Transfer*, 40(4), 973-986.
10. Gupta, D., Solanki, S.C., & Saini, J.S. (1997). *Thermohydraulic performance of solar air heater with roughened absorber plates*. *Solar Energy*, 61(1), 33-42.

11. Varshney, L. & Saini, J.S. (1998). Heat transfer and friction factor correlations for rectangular solar air heater duct packed with wire mesh screen matrices. *Solar Energy*, 62(4), 255-262.
12. Karwa, R., Solanki, S.C., & Saini, J.S. (1997). Heat transfer coefficient and friction factor correlations for the transitional flow regime in rib roughened rectangular ducts. *Int. J. Heat Mass Transfer*, 42, 1597-1615.
13. Karwa, R., Solanki, S.C., & Saini, J.S. (2001). Thermohydraulic performance of solar air heater having integral chamfered rib roughness on absorber plate. *Energy*, 26, 161-176.
14. Bhagoria, J.L., Saini, J.S., & Solanki S.C. (2002). Heat transfer coefficient and friction factor correlations for rectangular duct having transverse wedge shaped rib roughness on the absorber plate. *Renewable Energy*, 25(3), 341-369.
15. Sawant, S., More, S. E., & Dange, H. Design, Development and Performance Analysis of Anticorrosive Heat Exchanger.
16. Momin, A.M.E., Saini, J.S. & Solanki, S.C. (2002). Heat transfer and friction in solar air heart duct with V-shaped rib roughness on absorber plate. *J. Heat Mass Transfer*, 45(16), 3383-3396.
17. Sahu, M.M., & Bhagoria, J.L. (2005). Augmentation of heat transfer by using 90° broken transverse ribs on absorber plate of solar air heater. *Renewable Energy*, 30, 2057-2073.
18. Karwa, R. (2003). Experimental studies of augmented heat transfer and friction in asymmetrically heated rectangular ducts with ribs on the heated wall in transverse, inclined, V-continuous and V-discrete pattern. *International Communications in Heat Transfer*, 30(2), 241-250.
19. Jaurker, A.R., Saini, J.S., & Gandhi, B.K. (2006). Heat transfer and friction characteristics of rectangular solar air heater duct having rib-grooved artificial roughness. *Solar Energy*, 80, 895-960.
20. Aharwal, K.R., Gandhi, B.K., & Saini, J.S. (2009). Heat transfer and friction characteristics of solar air heater ducts having integral inclined discrete ribs on absorber plate. *Int. J. Heat Mass Transfer*, 52, 5970-5977.
21. Varun, Saini, R.P., & Singal, S.K. (2008). Investigation of thermal performance of solar air heater having roughness elements as a combination of inclined and transverse ribs on the absorber plate. *Renewable Energy*, 33, 1398-1405.
22. Senapati, N., & Dhal, R. K. (2013). Effect of Slip Condition on Unsteady MHD Oscillatory Flow in a Channel Filled with Porous Medium with Heat Radiation and Mass Transfer. *Int. J. Appl. Math. Stat. Sci*, 2(3), 11-20.
23. Saini, S.K., & Saini, R.P. (2008). Developments of correlations for Nusselt number and friction factor for solar air heater with roughened duct having arc-shaped wire as artificial roughness. *Solar Energy*, 82, 1118-1130.
24. Hans, V.S., Gill, R.S., & Singh, Sukhmeet. (2017). Heat transfer and friction factor correlations for a solar air heater duct roughened artificially with broken arc ribs. *Exp Thermal and Fluid Science*, 80, 77-89.
25. Gill, R.S., Hans, V.S., Saini, J.S., & Sukhmeet Singh. (2017). Investigation on performance enhancement due to staggered piece in a broken arc rib roughened solar air heater duct. *Renewable Energy*, 104, 148-162.
26. ASHRAE standard 93-97, Method of testing to determine the thermal performance of solar collector. 1991.